Turkish Journal of Physics

http://journals.tubitak.gov.tr/physics/

Research Article

Turk J Phys
(2019) 43: 472 – 480

doi:10.3906/fiz-1904-11

Topography of electrospun nanofibers and its influence on (POT/PS)/Si hybrid solar cell parameters

Tariq J. ALWAN*
Department of Physics, College of Education, Al Mustansiriyah University, Baghdad, Iraq

Received: 10.04.2019 • **Accepted/Published Online:** 21.08.2019 • **Final Version:** 21.10.2019

Abstract: Alignment nanofibers of poly(o-toluidine)/polystyrene (POT/PS) were prepared by using an electrospinning method at different applied voltages ($V_{appl.}$) of 10, 15, and 20 kV. The effect of the applied voltage on the morphology and electrical properties of POT/PS nanofibers was studied. Morphology and diameters of the nanofibers were investigated via atomic force microscopy. (POT/PS)/Si hybrid solar cells were fabricated through the deposition of POT/PS nanofibers on Si wafers using the electrospinning technique. The current-voltage measurements of the device under dark conditions exhibited asymmetrical and rectifying behavior for the Al/(POT/PS)/Si/Al junction, thereby confirming the formation of diodes. Diode parameters, such as ideality factor n* and saturation current I_o, were determined from the current density-voltage curves. The photovoltaic properties of the Al/(POT/PS)/Si/Al junction were studied under illuminated condition. Results revealed short-circuit current density J_{sc} = 1.45 mA, open-circuit voltage V_{oc} = 596 mV, and solar cell efficiency = 3.04.

Key words: Poly(O-toluidine), nanofibers, conducting polymer, electrospinning, hybrid solar cell

1. Introduction

One of the important structures of nanomaterials is 1D, which has a high surface area given the small diameter, and where the nanofiber films are highly porous with perfect pore interconnectivity. These distinctive characteristics, in addition to their polymer properties, make nanofibers widely used in advanced applications. The electrospinning method is considered the most promising process in producing nanofibers from a wide range of polymers, in which fiber diameter can be reduced from micrometers to nanometers [1]. Poly(o-toluidine) (POT) is similar to a polyaniline (Pani) derivative, which includes the -CH_3 group in the ortho position of the aromatic ring of the aniline monomer [2]. As a key conducting polymer, POT can be easily synthesized either chemically or electrochemically [3]. Polymer photovoltaics is an important discovery that solves many problems in traditional photovoltaic technologies. Its technology presents the possibility of fast processing, low cost, light weight, flexibility, and a low thermal budget [4]. Cells with two layers are used; one contains electron-accepting molecules, whereas the other contains electron-donating layers. The majority of the light is absorbed by the electron-donating layer and creates excitons. The excitons have to dissociate to form free-charge carriers. This process occurs at the two-layer interface, and the dissociation process is considerably enhanced due to the relatively high energy difference between these layers, having two individual layers separating the electron and hole transportation, thereby reducing recombination. Moreover, the active region where the splitting process

*Correspondence: tariqjaffer2000@yahoo.com

occurs extends into the accepting and the donating layers. Such a mechanism nearly doubles the active region compared with single-layer cells. Using two different semiconductors allows the band gaps to be tuned to match the solar spectrum [5]. Solar cells based on conducting polymer/wafer silicon (Si) have attracted broad research interest because of their advantages; however, conversion efficiency is still low [6]. The efficiency of solar cell heterojunctions depends on the physical interaction of the p-type and n-type layers, which is dependent on the layers' morphology, even if the p-type and n-type layers have an ideal electronic relationship [7,8]. In this study, an Al/(POT/PS)/Si/Al hybrid solar cell is fabricated using poly(o-toluidine)/polystyrene (POT/PS) nanofibers as a p-type layer on a Si wafer. The parameters of this hybrid solar cell and the effect of nanofiber morphology on the parameters are then explored.

2. Experimental

POT was synthesized by the oxidation polymerization of o-toluidine in acidic media in accordance with the previously described method of Alwan and Jalli [9]. POT powder (0.25 g) was dissolved in 10 mL of $CHC1_3$; afterwards, 3% weight ratio of PS was added to prepare a POT/PS solution. Then 3 mL of the solution was put into a feed tank (syringe), which included a metal needle. A high-voltage power supply (direct current) was connected at the end of the needle as an anode, with a rotated aluminum cylinder collector as a cathode. The processing conditions of the different applied voltages ($V_{appl.}$) of 10, 15, and 20 kV were as follows: the flow rate was 0.3 mL/h, the space between the collector and needle was 15 cm, and the needle diameter was 23 G. The glass slides and N-type Si wafer (111) were fixed on the surface of the moving collector. Figure 1 illustrates the hybrid solar cell structure. The surface morphologies of the nanofiber layers were tested via atomic force microscopy (AFM; AA3000 Angstrom Advanced Inc.). The dark and illumination currents of the junction at bias voltage (V_B) (–1 to 1) V in the case of forward and reverse bias connections were measured. A halogen lamp (Philips 100 W) was used in the illumination case.

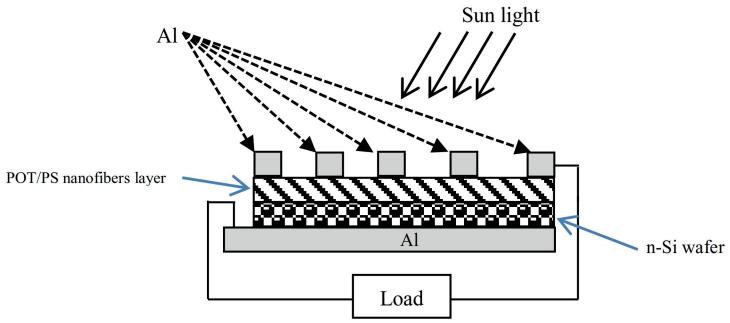

Figure 1. The hybrid solar cell.

3. Results and discussion

The POT/PS nanofibers were examined by SEM and AFM to identify their morphology, diameter, and alignment. Figure 2 shows the SEM image of POT/PS nanofibers at applied voltage $V_{appl.}$ of 10 kV. Figure 3 shows the AFM images of POT/PS nanofibers at different applied voltages ($V_{appl.}$) of 10, 15, and 20 kV. The electrospinning of nanofibers from POT soluble in $CHCl_3$ is impossible without the addition of PS to POT and dissolving in $CHCl_3$. No fiber formation occurred because the surface tension and the viscosity of the solution are not sufficiently high to maintain a stable drop at the end of the capillary tip. The SEM and AFM images

show that all cases have good aligned nanofibers. The figure also shows that the prepared samples are free of defects such as bubbles and reducers. The prepared nanofibers have a generally uniform thickness and are smooth. In addition, the obtained uniaxially aligned nanofibers and the alignment between the parallel fibers are constantly separated by large distances. The length of the nanofiber continues along the test area, which ends at 2 μm. From Figure 3 it is clear that as $V_{appl.}$ increases the average diameter of nanofibers decreases from 134.9 nm at $V_{appl.}$ of 10 kV to 19.6 nm at an applied voltage $V_{appl.}$ of 20 kV. In the electrospinning method, $V_{appl.}$ is a crucial factor; only when $V_{appl.}$ is higher than the threshold voltage can charged jets be ejected from the Taylor cone [10]. Many researchers have indicated that a high voltage leads to increased electrostatic repulsive force on the charged jet, which favors the reduction of fiber diameter [9].

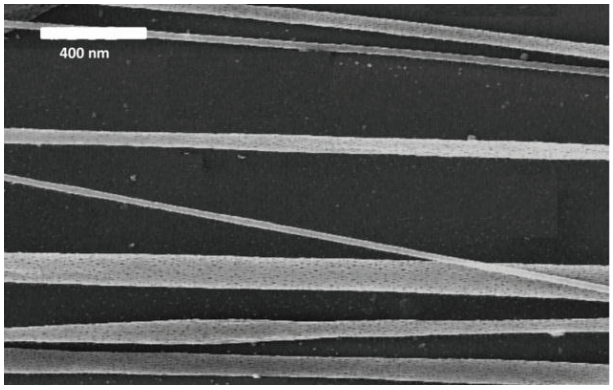

Figure 2. SEM image of POT/PS nanofibers at 10 KV V_{appl}.

Table 1 shows the electrical conductivity values of POT/PS nanofiber layers. Electrical conductivity of 3.11×10^{-5} S.cm^{-1} increases to 9.77×10^{-5} S.cm^{-1} when $V_{appl.}$ is raised from 10 kV to 20 kV. This increase in $V_{appl.}$ reduces the nanofiber diameter and enhances the structural properties, which is in line with the findings of Sarac [11] and Konagaya et al. [12].

Table 1. The parameters values of POT/PS nanofibers and the values of n*, J_s, and $\Phi_{b.}$ of Al/(POT/PS)/Si/Al devices.

$V_{appl.}$, kV	Aver. d, nm	σ, S cm^{-1}	J_s, A/cm^2	n*	Φ_b eV
10	134.9	3.11×10^{-5}	8.22×10^{-6}	2.88	0.701
15	95.3	7.39×10^{-5}	3.37×10^{-6}	3.01	0.689
20	19.6	9.77×10^{-5}	1.88×10^{-6}	3.76	0.665

The results of the current-density-voltage (J–V_B) measurements in forward and reverse modes under darkness and illumination for Al/(POT/PS)/Si/Al devices and the parameters of ideality factor n*, short-circuit current (J_{sc}), and open-circuit voltage (V_{oc}) will be discussed.

The forward dark current is generated when applied voltage V_B in the holes in the p-type region (POT/PS nanofiber in the current study) and the electrons in the n-type region (Si wafer in the current study) are pushed towards the junction. This process reduces the width of the depletion zone and the value of built-in potential. The forward dark current curve is divided into two regions, low- and high-voltage regions, depending on the conduction mechanism of the current [13,14].

At reverse bias, the curve has two regions. The first one is the generation region (low-voltage region,

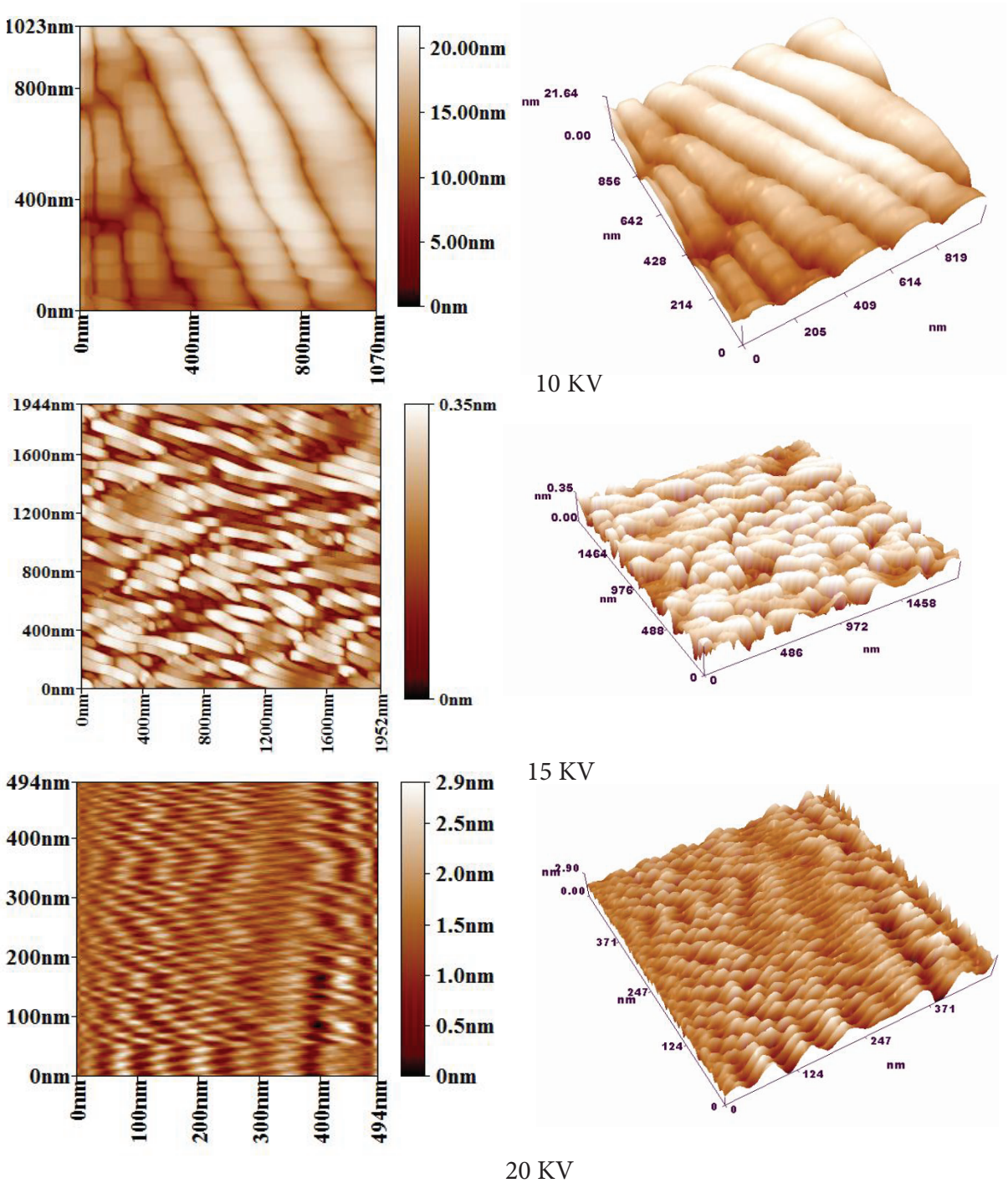

Figure 3. AFM images of POT/PS nanofibers at different V_{appl}.

V_B $< 0.3\ V_B$), where the reverse current is lightly increased with V_D and tends to generate electron-hole pairs. In the second region (high-voltage region, $V > 0.3$ V), a considerable increase in the reverse bias can be recognized. In this case, the current results from the diffusion of minority carriers through the (POT/PS)/Si junction [14].

Figure 4 shows that the value of forward current density under darkness is increased with $V_{appl.}$ (decreasing of nanofiber diameter) in Al/(POT/PS)/Si/Al. This effect is attributed to the decrease in the depletion zone width because of the improvement in the structure and increased conductivity of POT/PS at small diameters.

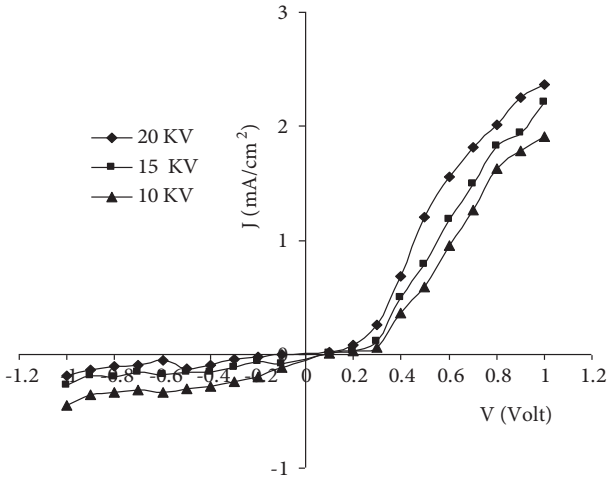

Figure 4. Relations of (J-V) under dark conditions for Al/(POT/PS)/Si/lA at different V_{appl}.

Information about the conduction mechanisms can be obtained from (J-V) characteristics curves. Figure 5 shows the semilogarithmic curves of the forward J-V for the Al/(POT/PS)/Si/Al hybrid at room temperature. These curves include two regions, which refer to different conduction mechanisms. The first region is at low-forward voltage ($\cong$ VB $\leq$ 0.4 V) and the conduction mechanism of current in this region is described by the recombination or diffusion and emission model [15].

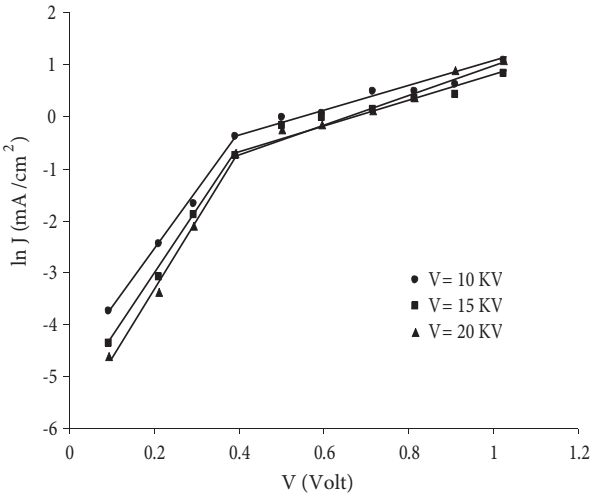

Figure 5. The ln (J-V) characteristics at forward bias voltage for Al/(POT/PS)/Si/Al at different V_{appl}.

The relation between voltage and the junction current can be simplified as follows [16]:

$$\ln \mathrm{J} \;=\; \ln \mathrm{J_s} + \left(\frac{\mathrm{qV}}{\mathrm{n^{*}K_B\,T}} \right) \tag{1}$$

where J_s is the saturation current and is expressed as:

$$J_s = A^* T^2 \exp\left(\frac{q\Phi_b}{K_B T}\right) \tag{2}$$

where A* is the Richardson constant and equal to 120 A/cm^{-2} K^{-2}, and Φ_b is the barrier height of the heterojunction.

The saturation current can be obtained by extrapolation of the linear ln(J)-V portion to the ln(J) axis at zero voltage. Parameters J_s and n* can be readily determined from the curve shown in Figure 5 together with Eq. (1). Table 1 lists the values of J_s and n*. The value of the ideality factor varies between 2.88 and 3.67, and this finding is in agreement with that of Boyarbay et al. [17], who found that the value of n* is approximately 2.31 for a Pani/TiO_2/p-Si heterojunction.

Often the value of n* is close to one. The high values of n* (n* > 2) in the prepared junctions may be attributed to different factors such as leakage, interfacial layer thickness, shunting, bulk series resistance, or any resistive loss [16].

In the second region (high voltage), another conduction mechanism seems to be predominant. The current shows a power dependence of voltage. This power dependence suggests that the dark current is space-charge-limited current-dominated [15].

Table 1 also includes the values of barrier height Φ_b, which depend on Eq. (2).

Figure 6 show the relationship between the photocurrent and bias voltage V_D in the range of [–1 to 1] V for Al/(POT/PS)/Si/Al with different V_{appl}. The measurements are achieved at a power intensity of illumination 100 mW/cm^2. The photocurrent is considered a significant parameter, which plays an effective role in solar cells.

When a solar cell is illuminated, the generated electron-hole pairs strongly increase. By contrast, the resistivity of samples decreases with illumination. This finding indicates that excess carriers increase conductivity and the mobility of the carriers.

Figure 6 and Table 2 show that the J_{ph} of Al/(POT/PS)/Si/Al increases from 1.01 mA/cm^2 to 1.45 mA/cm^2 when $V_{appl.}$ increases from 10 kV to 20 kV. This result is attributed to the effect of the increase in conductivity, which reduces the mean free path of carriers, thereby increasing J_{ph}. Moreover, this result is in agreement with researchers who assert that J_{ph} increases with conductivity [18].

Table 2. The parameters of Al/(POT/PS)/Si/Al solar cell.

$V_{appl.}$ KV	V_{oc} (mV)	J_{sc} (mA/cm^2)	V_{max} (mV)	J_{max} (mA)	P_{max} (mW/cm^2)	FF	η%
10	500	1.01	255	0.56	142.8	0.28	1.42
15	542	1.3	351	0.83	290.5	0.41	2.90
20	569	1.45	380	0.8	304	0.36	3.04

Table 2 shows the relationship between short-circuit current J_{sc} and open-circuit voltage V_{oc} at different values of V_{appl}.

The short-circuit current J_{sc} is referred to as photocurrent J_{ph} because a current without any external bias voltage V_D exists as if a short circuit occurs in the system [18].

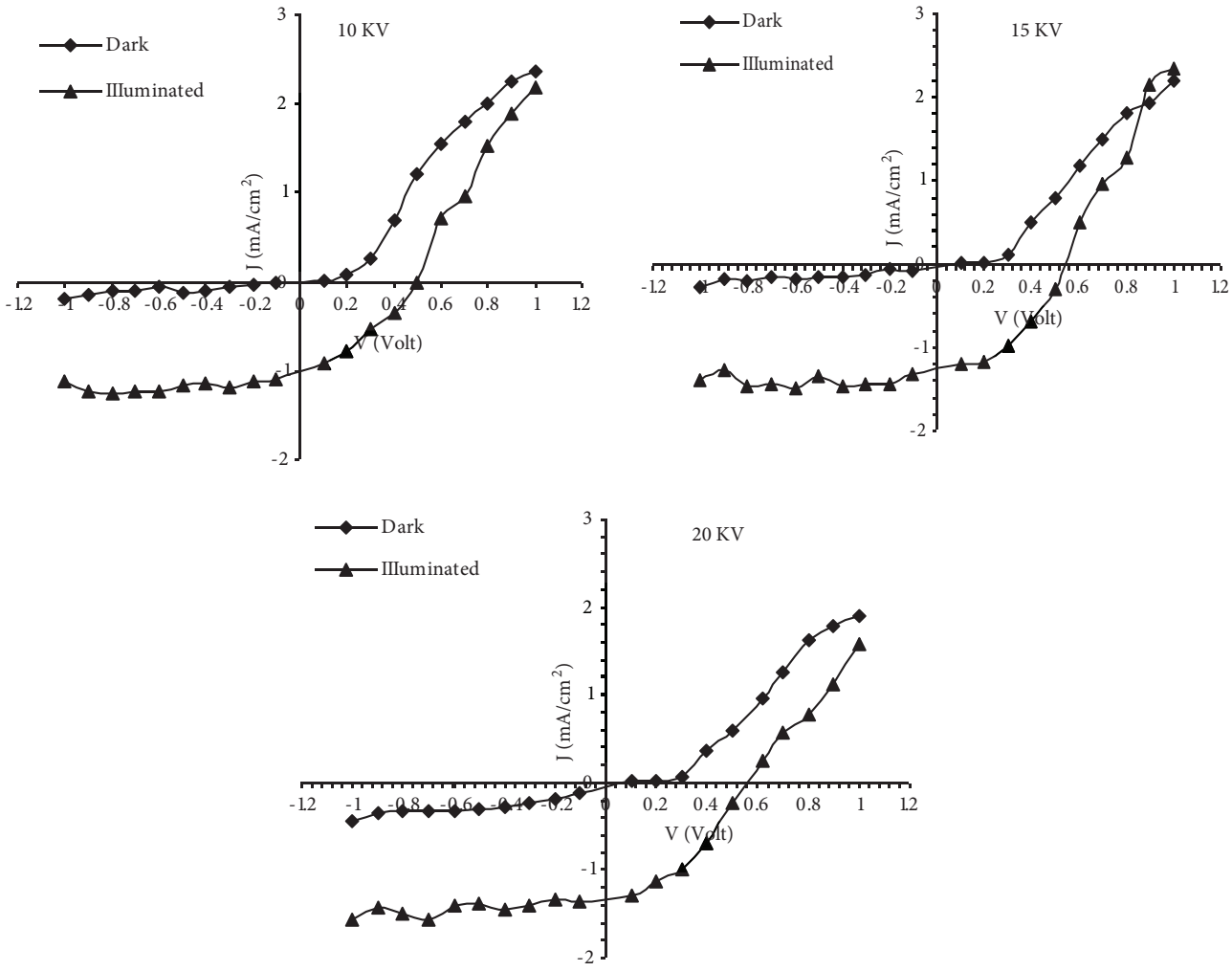

Figure 6. The relations of (J-V) under dark and illumination for Al/(POT/PS)/Si/lA at different V_{appl}.

From the obtained result, a systematic increase is observed between V_{oc} and the increasing $V_{appl.}$ in devices. This increase occurs due to the improvement in crystal structure and rising conductivity of POT/PS with the increase in V_{appl}. This finding is in an agreement with that of Wang et al. [19], who found that V_{oc} increases with conductivity for Pani on crystalline Si hybrid solar cells.

The fill factor (FF) for Al/(POT/PS)/Si/Al is calculated as:

$$FF = \frac{P_{max}}{V_{oc}.I_{sc}} = \frac{V_{max}.I_{max}}{V_{oc}.I_{sc}}, \tag{3}$$

where P_{max} is the maximum electrical power obtained [20].

The efficiency of a solar cell η is measured as the fraction of incident power converted to electricity and is defined as follows:

$$P_{max} = V_{oc}.I_{sc}.FF, \tag{4}$$

$$\eta = \frac{P_{max}}{P_{in}}. \quad (5)$$

The maximum power produced by a solar cell depends on the FF. Therefore, FF is an important parameter that determines the power conversion efficiency of a hybrid solar cell. Several factors can considerably influence FF. These factors intricately interact with one another. Thus, a deep understanding of FF is difficult to achieve [21], and from these factors, voltage drops because of shunt resistance R_{sh}, series resistance R_s and the recombination in a nonideal solar cell [22].

Table 2 shows that the FF and conversion efficiency increase with $V_{appl.}$, which decreases the nanofiber diameter, changes the morphology of the nanofiber layer, and increases conductivity.

4. Conclusion

An organic-inorganic hybrid solar cell based on POT nanofiber and Si wafer was fabricated using an electrospinning technique. The I–V characteristics of this junction have a rectifying effect, which is interpreted in terms of the barrier formation at the (POT/PS)/Si interface. The prepared solar cell at 20 kV shows better conversion efficiency of 3.04 compared with that of the solar cell at 10 kV with 1.42.

References

[1] Seeram R, Kazutoshi F, Wee-Eong T. An Introduction to Electrospinning and Nanofibers. Singapore: World Scientific Publishing Co. Pte. Ltd., 2005.

[2] Zaidan KM, Talib RA, Rahma MA, Khaleel FH. Synthesis and characterization of poly(o-toluidine) POT blend with polyethylene oxide PEO as conducting polymer alloys. Der Chemica Sinica 2012; 3 (4): 841-848.

[3] Tursun A, Zhang X, Ruxangul J. Synthesis and characterization of poly(o-toluidine) doped with organic sulfonic acid by solid-state polymerization. Journal of Applied Polymer Science 2005; 96: 1630-1634. doi: 10.1002/app.21614

[4] Frederik CK. Polymer Photovoltaics: A Practical Approach. Bellingham, WA, USA: Society of Photo-Optical Instrumentation Engineers Press, 2008.

[5] Hu W, Bai F, Gong X, Zhan X, Fu H et al. Organic Optoelectronics. Weinheim, Germany: Wiley-VCH, 2012.

[6] Ziadan KM. Conducting polymers application. In: De Souza Gomes A (editor). New Polymers for Special Applications. Rijeka, Croatia: InTech, 2012. pp. 3-24.

[7] Benanti TL, Venkataraman D. Organic solar cells: an overview focusing on active layer morphology. Photosynthesis Research 2006; 87: 73-81. doi: 10.1007/s11120-005

[8] Thompson BC, Frechet JMJ. Polymer–fullerene composite solar cells. Angewandte Chemie International 2008; 47: 58-77. doi: doi.org/10.1002/anie.200702506

[9] Tariq JA, Fatima SJ. Structure and electrical properties of Pani.CSA/PMMA nanofibers prepared by electrospinning method. Optoelectronics and Advanced Materials – Rapid Communications 2018; 12 (1-2): 100-107.

[10] Darunee A. Electrospun conducting nanofiber–based materials and their characterizations: effects of fiber characteristics on properties and applications. PhD, University of Akron, Akron, OH, USA, 2006.

[11] Sarac AS. Nanofibers of conjugated polymer composites. Journal of Nanomedicine & Nanotechnology 2012; 3 (9): 77-78. doi: 10.4172/2157-7439.S1.003

[12] Konagaya S, Shimizu K, Terada M, Yamada T, Sanada K et al. Effect of diameter of cellulosic nano-fiber on conductivity of poly(aniline sulfonic acid) composites. In: 29th International Conference of the Polymer Processing Society; Nuremberg, Germany; 2014. pp. 270-273. doi: 10.1063/1.4873779

[13] Shah M, Karimov K, Ahmad Z, Sayyad MH. Electrical characteristics of Al/CNT/NiPc/PEPC/Ag surface-type cell. Chinese Physics Letters 2010; 27 (10): 106102. doi: 0.1088/0256-307X/27/10/106102

[14] Sharma BL, Purohit RK. Semiconductor Heterojunctions. First Edition. Oxford, UK: Pergamon Press, 1974.

[15] El-Nahass MM, Atta AA, El-Sayed HE, El-Zaidia EFM. Electrical transport mechanisms and photovoltaic characterisation of MgPc/p-Silicon hybrid organic–inorganic solar cells. Current Organic Chemistry 2010; 14 (1): 84-88. doi: 10.2174/138527210790226447

[16] Farag AM, El-Shazly EAA, Abdel Rafea M, Ibrahim A. Optical, electrical and photovoltaic characteristics of organic semiconductor based on oxazine/n-Si heterojunction. Solar Energy Materials & Solar Cells 2009; 93 (10): 1853-1859. doi: 10.1016/j.solmat.2009.06.023

[17] Boyarbay B, Cetin H, Uygun A, Ayyildiz E. Electrical characterization and fabrication of organic/inorganic semiconductor heterojunctions. Applied Physics A 2011; 103 (1): 89-96. doi: 10.1007/s00339-011-6305-4

[18] Wurfel P. Physics of Solar Cells: From Principles to New Concepts. Weinheim, Germany: Wiley-VCH, 2005.

[19] Wang W, Schiff EA. Polyaniline on crystalline silicon heterojunction solar cells. Applied Physics Letters 2007; 91 (13): 133504. doi: 10.1063/1.2789785

[20] Byranvand MM, Kharat AN, Fatholahi L. Influence of nanostructured TiO_2 film thickness on photoelectrode structure and performance of flexible dye-sensitized solar cells. Journal of Nanostructures 2012; 2 (3): 327-332. doi: 10.7508/JNS.2012.03.009

[21] Qi B, Wang J. Fill factor in organic solar cell. Physical Chemistry Chemical Physics 2013; 15 (23): 8972-8982.

[22] Al Abdullah K, Al Alloush F, Ali J, Salame C. Study of the effects related to the electric reverse stress currents on the mono-Si solar cell electrical parameters. Energy Procedia 2013; 36: 104-113. doi. 10.1016/j.egypro.2013.07.013